Evaluation of Array Antenna Systems for GNSS Applications Using Wave-Field Synthesis in an OTA Laboratory

Christopher Schirmer[1,2], Alexander Rügamer[2], Wim A. Th. Kotterman[1],
Markus H. Landmann[2], Giovanni Del Galdo[1,2]
[1]Technische Universität Ilmenau, Helmholtzplatz 2, 98684 Ilmenau, Germany
[2]Fraunhofer Institute for Integrated Circuits IIS, Am Wolfsmantel 33, 91058 Germany

***Abstract*—Antenna characterization is usually performed by antenna pattern measurements in an anechoic chamber. Subsequently, a conducted test, the Radiated Two-Stage (RTS) or the Wireless-Cable method can be used for an overall system test considering the measured patterns.**

In this paper we present a method to perform device tests for antenna arrays / smart antennas without the need of radiation pattern measurements, and we validate it experimentally. By using Over-The-Air tests in a Virtual Electromagnetic Environment and Wave-Field Synthesis, the propagation environment can be realistically recreated in the region around a Device-Under-Test. This allows for reproducible performance comparisons of different antennas or systems under identical propagation environment conditions. As a special application, we consider the Controlled Reception Pattern Antenna (CRPA) in a Global Navigation Satellite Systems environment in the presence of interferer signals.

***Index Terms*—CRPA, GNSS, GPS, OTA, WFS**

I. Introduction

In communication systems, such as Long Term Evolution (LTE), or Global Navigation Satellite Systems (GNSS), device tests are aimed at ensuring proper functioning. This not only includes throughput (MIMO/LTE devices), or received signal quality (GNSS case), but also robustness against in-band or inter-system interference. Due to the inherently low power of GNSS signals (≈-127 dBm received signal power on earth), the GNSS bands are dominated by white Gaussian noise. The noise is about hundred to a few thousand times stronger than the GNSS signal itself. As a consequence, the GNSS signals are extremely susceptible to all types of interference. Commercial Off The Shelf (COTS) radios are available cheaply, sold as so-called *privacy protection devices* to prevent positioning [1]. Such devices cause powerful in-band interference, which can be mitigated by the use of Controlled Reception Pattern Antennas (CPRAs) and adequate signal processing algorithms.

Different test procedures are available, namely the Radiated Two Stage (RTS), or the Wireless Cable (WLC) method [2], [3]. All mentioned methods require the device antenna array radiation pattern to be measured before testing.

In this context, we proposed the Over-The-Air testing in a Virtual Electromagnetic Environment (OTAinVEE) using Wave-Field Synthesis (WFS, [4]–[6]) at the Facility for Over-the-air Research and Testing (FORTE, [7]) as an alternative. OTAinVEE using WFS allows for accurate spatial emulation of a wireless propagation channel, arbitrary kinds of tests and propagation environments can be emulated. WFS omits the need for pattern measurements as the propagation environment is reproduced as in reality. To the authors knowledge, no practical test case of the OTAinVEE WFS method for device testing and evaluation was demonstrated before. Hence, this paper presents an insight into ongoing activities in the area of WFS for the characterization of CRPA antennas at Technische Universität Ilmenau and Fraunhofer IIS, and provides a detailed description and analysis for OTAinVEE performance measurements.

This paper is organized as follows. The applied scenario for the CRPA performance measurements is explained in Section II, followed by the evaluation metrics in Section III, and the needed signal processing in Section IV. In Section V, the measurement setup with the implementation is described. The results are discussed in VI. Section VII concludes the paper.

II. Scenario

In this paper, the vulnerability of GNSS reception with respect to interference is under investigation, using a 4-elements CRPA including a 4-channel data recorder and a software receiver. The system exposed to real-world conditions including a realistic interferer profile. The interferer influence on system performance is evaluated using three methods:

- Usage of only one antenna element (single antenna equivalent)
- Application of Null Steering (NL) to the digital base-band (DBB) signal of the four receiver chains
- Application of Beam Forming (BF) to the DBB signal of the four receiver chains

By using the Spirent GSS9000 TS788 GNSS RF Constellation Simulator (RFCS), the receiver is emulated at Lon./Lat. $0°/0°$ using ten GPS satellite signals. The spatial distribution of the satellites is emulated using the WFS system at FORTE.

978-88-907018-7-0/17/$31.00 ©2017 IEEE

#1570318339

According to the satellite Co-elevation, each signal is emulated at its actual position relative to the receiver CRPA, cf. Figure 1, [6].

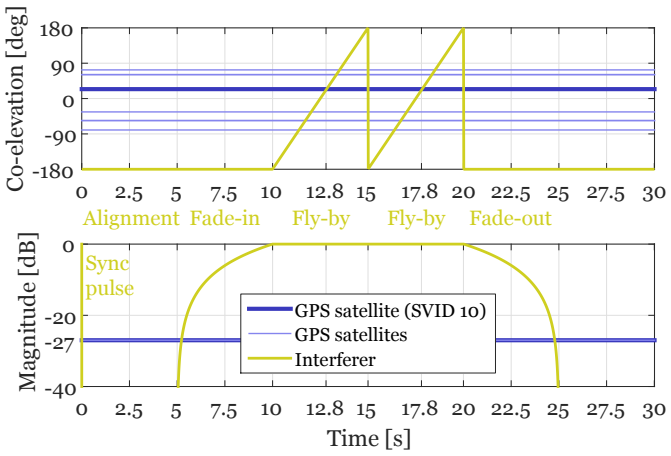

Fig. 1. Motion and magnitude profile of GPS satellites and interferer signal.

In the realistic case of a mobile DUT or interferer, its movement profile is modeled in 4 phases (lime green lines). After a sync pulse, used for measurement data synchronization, a GPS alignment phase starts that allows the receiver to track the signals by locking the tracking loops. After that, the interferer begins to fade in at the back side of the DUT CRPA. Two fly-byes are emulated where the interferer circulates around the antenna, before it fades out at the end. The practical implemented interferer has a bandwidth of 5 MHz and is realized as a Crest-factor optimized multi-sine signal [8].

III. Analysis Metric

In the GNSS context, the final result is the positioning and its accuracy. As the positioning accuracy is strongly influenced by the satellite constellations and receiver algorithms, we use an intermediate metric that allows to directly analyze the received signal quality of individual GPS satellite signals, the carrier-to-noise-density ratio for a selected satellite. The C/N_0 is an important metric that helps GNSS receivers to quantify the reliability of a received signal and is proportional to the obtained position estimate, and therefore, to a position estimate. Commonly used algorithms for the C/N_0 estimation are for example Bealueu's method [9], the Narrow-Wideband Power Ratio (NWPR) method [10], and the Moments Method (MM) [11]. In this paper, we employ the MM as it has low implementation complexity, and is designed to operate well at low SNR regimes [12], which is the case with interferer presence because unwanted signals are considered as noise.

IV. Signal Post-Processing

Several algorithms for NL and BF are available in the literature. Here the focus is not on the performance of the algorithms but on the demonstration of the proposed WFS testing method. This includes different configurations of a GNSS receiver with one or more receiver chains.

A. Single Antenna Element

In the case of only a single CRPA element used, the DBB signal is directly passed to the software GPS receiver for acquisition and tracking.

B. Null Steering

Null Steering is the form of signal processing, in which no knowledge of the antenna pattern is available. It detects the interferer signal and places a null in the respective direction. The optimum steering weights $\boldsymbol{w}_{\text{opt,NL}}$ for the DBB signals are obtained by $\text{Null}\{\boldsymbol{b}_\text{i}^\text{T}\} \cdot \boldsymbol{\lambda}$, with $\lambda_1, \lambda_2, \ldots \lambda_{M-1} = 1$, where $\text{Null}\{\cdot\}$ is the null-space operator to determine the orthogonal space to the antenna response in interferer direction $\boldsymbol{b}_\text{i}^\text{T}$. The vector $\boldsymbol{b}_\text{i}^\text{T}$ is determined using the measurement data which means that no radiation pattern information is needed. The value $\boldsymbol{\lambda}$ is a scaling of the orthogonal base vectors and is set to ones as a simplification.

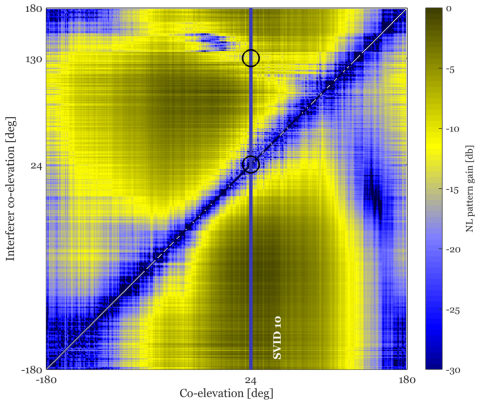

Fig. 2. Measured CRPA radiation pattern after NL, azimuth $\phi = 0°/180°$.

When NL is applied there is no control of the additional nulls, that are unavoidable with a multi-element antenna. Therefore, Figure 2 shows a simulation for the resulting radiation pattern of the array antenna, that is used in the following investigations, for all possible interferer incidence co-elevation angles (azimuth $\phi = 0°/180°$). Desirable are nulls at the angle bisector. Additional signal fades can be seen at around 170° for jammer incidence angles up to 80°, also at an interferer angle of 130° (black upper circle). As this behavior for NL is unavoidable, we profit from the multiple available satellites in a GNSS system. It is unlikely to interfere at all angles of satellites necessary for positioning as they are distributed over the sky, which is accordingly emulated using WFS. The blue line denote the investigated satellite with Space Vehicle ID (SVID) 10.

C. Beam Forming

In the case of BF, we apply the method proposed in [13], [14]. The optimal weights are obtained by

$$\boldsymbol{w}_{\text{opt,BF}}^{H} = \boldsymbol{g}^{H} \left(\boldsymbol{C}^{H} \boldsymbol{R}^{-1} \boldsymbol{C}\right)^{-1} \boldsymbol{C}^{H} \boldsymbol{R}^{-1}, \qquad (1)$$

where $\boldsymbol{R}$ is the covariance matrix of the processed DBB signals, $\boldsymbol{C} = [\boldsymbol{b}_\text{i}, \boldsymbol{b}_\text{d}]$ the constraint matrix with the radiation

pattern vectors of the interfering (i), and the desired (d) signal incidence angles. The gain vector $\boldsymbol{g} = [g_\mathrm{i},\ g_\mathrm{d}] = [0,\ 1]$ prescribes the attenuation (0) or amplification (1) of the specific signal incidence angles.

V. Measurement Setup and Implementation

Figure 3 shows a schematic of the used setup. Ten GPS satellite signals are emulated by the RFCS, and the interferer raw signal is generated using an arbitrary wave-form generator (ARB). The DBB signals are forwarded to the 12×24 OTA channel emulators with a maximum connectivity of 12×36. There, the convolution of the 12 input signals with the 12×24 WFS weights for all OTA antennas according to signal incidence angle takes place. All signals are DA-converted and mixed to the operating frequency of $1.575,42\,\mathrm{GHz}$ for the GPS L1 band. The signals are radiated by the OTA antennas, mounted on a 2D OTA ring, towards the CRPA DUT. At the DUT-side, the signals are recorded using 2 Flexiband recorders [6], [15]. The recorded DBB signals are processed in Matlab by the explained signal processing algorithms, and evaluated by a software GPS receiver implementation of Fraunhofer.

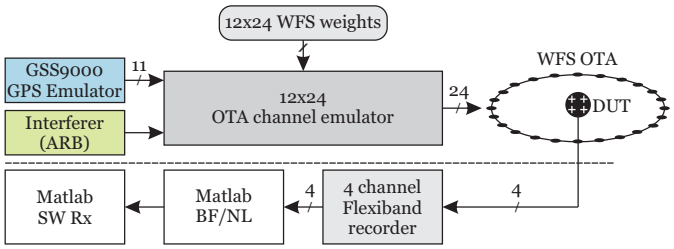

Fig. 3. Schematic of OTAinVEE WFS hardware.

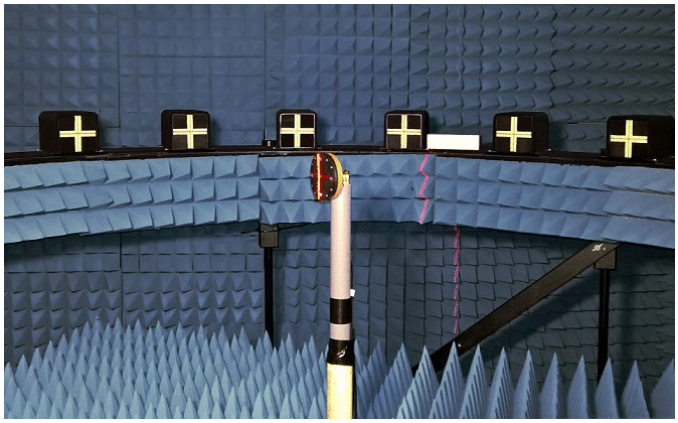

Fig. 4. Antcom 4-elements CRPA mounted in the OTA testbed [16, p. 50].

The measurement setup is depicted in the Figures 4 and 5. The 4-element CRPA, manufactured by Antcom [16], is mounted in the sweet spot area inside the anechoic chamber. The DBB measurement data is stored at the hard drives of two Laptops, which are connected to the receivers via USB 3.0. The four data streams are stored with a resolution of 8 bit I/Q sampled at 10.125 MHz providing a RF bandwidth of $\approx$10 MHz. 8 bit allow for a dynamic range of approximately 48 dB, which constrains the GPS and interferer power ratios. The satellite powers are emulated to result in C/N_0 values between 45 dBHz and 50 dBHz depending on the satellite elevation for the interferer free case. The interferer has a power level 27 dB above the GPS signals to keep a safety margin within the receiver dynamic range.

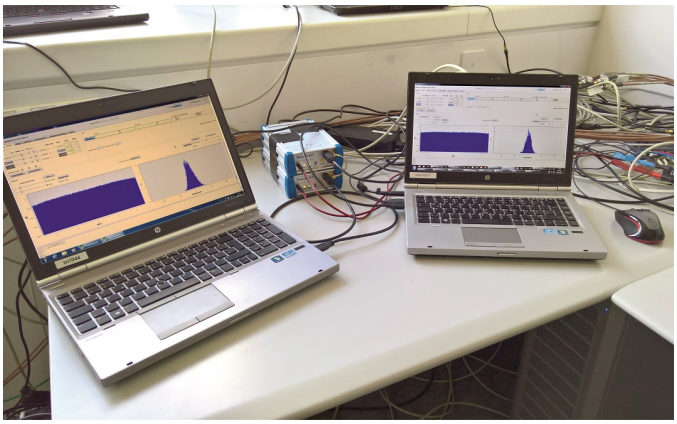

Fig. 5. Receiver hardware: Two synchronized Flexiband receivers (2×3 channels), with each having one laptop running a signal analysis and recording software.

By using a 2D OTA ring, a two-dimensional WFS can be performed. The GPS satellite co-elevation angles are equivalent to OTA azimuth angles, when the DUT CRPA is positioned upright. Satellite azimuth angles are mapped to the closest position on the OTA ring, cf.Figure 6.

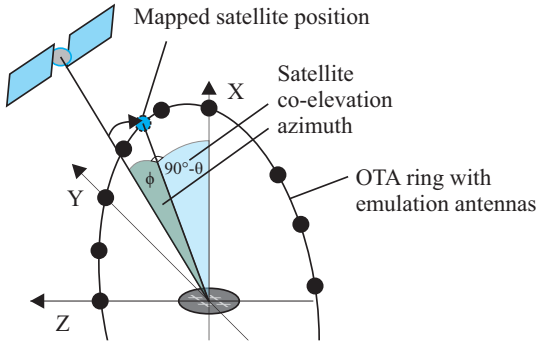

Fig. 6. Mapping of satellite azimuth and elevation to OTA coordinate system.

Prior to measurement and calibration, a simulation is performed to analyze the achievable WFS quality for the investigated DUTs. Beside the achievable field quality, the distribution, and the number of optimization points for the calibration is determined. Further information can be found in [5].

After determination of the optimal calibration points constellation, a field probe is mounted at the positioner inside the OTA ring center measuring the field of each OTA emulation antenna at each optimization point. The result of $M \times N$ measurement points for M emulation antennas times N optimization points is called transfer matrix and used to determine

the steering vector lookup-table for each signal incidence angle on the OTA ring. Detailed information for the steering vector determination can be found in [5].

After removal of the field probe, the CRPA is aligned to the center of the OTA ring coordinate system with the help of a 3-axis laser cross (cf. Figure 4). For all input signals, ten satellite signals and one interferer signal, the needed steering vectors according to the profile shown in Figure 1 are loaded into the OTA channel emulator, responsible for all OTA emulation antennas. The Flexiband signal recording is started, and the interferer/GPS motion profiles are replayed synchronously with the RFCS satellite emulation is launched.

For the case of the investigation of multiple CRPAs under identical conditions it has to be ensured, that the EVM sweet spot analysis is valid for all antenna dimensions, and the same calibration data (lookup-table) are used.

VI. Evaluation

The results of the CRPA analysis are depicted for the relevant part of the measurement between 5 and 20 seconds, see Figure 7. The top plot shows the C/N_0 values for SVID 10 while the bottom plot shows the correlator output for the different algorithms. The black curve, denoting the single element analysis, starts with around 50 dBHz and decreases to 38 dBHz when the interferer passes the satellite incidence angle. Even without NL or BF the tracking does not interrupt, due to the relatively weak jammer signal. The NL curve (blue) has a very different behavior. Until 8 s, the C/N_0 is above 50 dBHz. Then the interferer signal power exceeds the threshold for turning on NL/BF. Due to noisy effects around the threshold, a 10 dBHz fade occurs for NL. The signal then rises again above 50 dBHz until the interferer crosses the satellite signal incidence angle. After the drop at 12.8 s, another drop appears at 14.1 s, due to uncontrolled additional nulls in the resulting CRPA pattern (Figure 2, black circles). At 17.8 s and 19.4 s similar happens as the interferer takes the second turn. BF (lime curve), is similarly effected, when the interferer coincides with the GPS satellite direction. Due to additional focusing of the desired signal, very good C/N_0 values are achieved otherwise. The bottom plot showing the real part of the correlator output gives an impression of the navigation symbols. The GPS software receiver uses a Costas phase tracking loop for its carrier tracking, which is insensitive for $180°$ phase shifts. This leads to the different navigation symbol phases seen in Figure 7. Moreover, at the interception points with the interference signal (12.8 s and 17.8 s) one can also see that the phase tracking is lost and recovers, however, now the phasing between BF and NL changed by $180°$.

VII. Conclusions

A method to evaluate the performance of CRPA antennas in connection with a multi channel GNSS receiver by using Over-The-Air testing in a virtual electromagnetic environment (OTAinVEE) using wave-field synthesis (WFS) is presented. It was shown, that by emulation of the spatial characteristics of GPS signals and interferer, it is possible to test the performance of signal processing algorithms in connection with CRPAs. This paper focuses on the testing process. By exposing different CRPAs to identical and realistic fields in the anechoic chamber, it was demonstrated that performance differences can be measured for arbitrary and also integrated antenna arrays without the need of measuring the antenna patterns in advance. As an example, a small CRPA with an element distance of $\lambda/6$ was used. With larger aperture size and less coupling between the elements, better performance of Null-Steering and Beam-Forming is expected. A larger aperture will result in smaller C/N_0 fades.

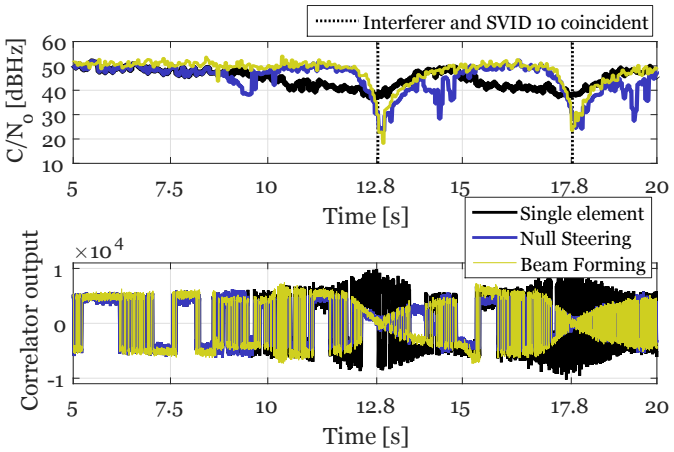

Fig. 7. C/N_0 values of SVID 10 (top), and corresponding corerlator output (bottom) for the three different signal processing methods: single element, BF, and NL.

Acknowledgment

The authors would like to thank the administration and members of Thüringer Innovationszentrum Mobilität (ThIMo) and the VISTA4F ProExzellenz research group funded by the Thuringian Ministry for Economic Affairs, Science, and Digital Society, in the context of which this research was performed.

References

[1] JAMMER4U.CO.UK. (2015) Handheld antitracking gps jammer. [Online]. Available: http://www.jammer4uk.com/handheld-antitracking-gpsl1-l2l3l4l5-jammer-j242g-p-29.html

[2] M. Rumney, H. Kong, Y. Jing, Z. Zhang, and P. Shen, *Recent advances in the radiated two-stage MIMO OTA test method and its value for antenna design optimization*, in *2016 10th European Conference on Antennas and Propagation (EuCAP)*, April 2016.

[3] C. Schirmer, M. Lorenz, W. A. T. Kotterman, R. Perthold, M. Landmann, and G. Del Galdo, *MIMO Over-The-Air testing for electrically large objects in Non-Anechoic environments*, in *The 10th European Conference on Antennas and Propagation (EuCAP 2016) (EuCAP 2016)*, Davos, Switzerland, Apr. 2016.

[4] W. Kotterman, M. Landmann, A. Heuberger, and R. Thomä, *New laboratory for over-the-air testing and wave field synthesis*, in *General Assembly and Scientific Symposium, 2011 XXXth URSI*, Aug 2011.

[5] C. Schirmer, M. Landmann, W. Kotterman, M. Hein, R. Thomä, G. Del Galdo, and A. Heuberger, *3D wave-field synthesis for testing of radio devices*, in *Antennas and Propagation (EuCAP), 2014 8th European Conference on*, April 2014, pp. 3394–3398.

[6] A. Rügamer, C. Schirmer, M. Lorenz, S. Taschke, M. Grossmann, M. Landmann, and W. Felber, *Setup and verification of a multi-GNSS over-the-air wave field synthesis testbed*, in *2016 IEEE/ION Position, Location and Navigation Symposium (PLANS)*, April 2016, pp. 863–873.

[7] (2015) FORTE – Facility for Over the Air Research and Testing. Fraunhofer Institute for Integrated Circuits IIS. [Online]. Available: http://www.iis.fraunhofer.de/de/abt/dvt/forte.html

[8] D. Gimlin and C. Patisaul, *On minimizing the peak-to-average power ratio for the sum of N sinusoids*, Communications, IEEE Transactions on, vol. 41, no. 4, pp. 631–635, Apr 1993.

[9] N. C. Beaulieu, A. S. Toms, and D. R. Pauluzzi, *Comparison of four SNR estimators for QPSK modulations*, IEEE Communications Letters, vol. 4, no. 2, pp. 43–45, Feb 2000.

[10] J. J. Spilker Jr., P. Axelrad, B. W. Parkinson, and P. Enge, *Global Positioning System: Theory and Applications*. American Institute of Aeronautics and Astronautics, 1996, vol. 1.

[11] D. R. Pauluzzi and N. C. Beaulieu, *A comparison of SNR estimation techniques in the AWGN channel*, in *Communications, Computers, and Signal Processing, 1995. Proceedings., IEEE Pacific Rim Conference on*, May 1995, pp. 36–39.

[12] E. Falletti, M. Pini, and L. L. Presti, *Low complexity carrier-to-noise ratio estimators for GNSS digital receivers*, IEEE Transactions on Aerospace and Electronic Systems, vol. 47, no. 1, pp. 420–437, January 2011.

[13] A. Konovaltsev, F. Antreich, and A. Hornbostel, *Performance Assessment of Antenna Array Algorithms for Multipath and Interference Mitigation*, in *2nd Workshop on GNSS Signals & Signal Processing - GNSS SIGNALS 2007*, 2007.

[14] H. L. Van Trees, *Optimum Array Processing (Detection, Estimation, and Modulation Theory, Part IV)*. Wiley-India, 2002.

[15] A. Rügamer, F. Förster, M. Stahl, and G. Rohmer, *A Flexible and Portable Multiband GNSS Front-end System*, in *Proceedings of the 25th International Technical Meeting of the Satellite Division of the Insitute of Navigation, ION GNSS 2012, September 17-21, 2012, Nashville, Tennessee, USA*, September 2012.

[16] Antcom. L1/L2 GPS GLONASS CRPA antennas. ANTCOM CORPORATION. [Online]. Available: http://antcom.com/documents/catalogs/05_Antcom_CRPA_L1L2_GPS_Antenna_Array_for_E_mailing.pdf